Failure Analysis of a Kaplan Turbine Runner Blade by Metallographic and Numerical Methods

DOINA FRUNZAVERDE
Center for Research in Hydraulics, Automation and Thermal Processes – CCHAPT
"Eftimie Murgu" University of Resita
P-ta Traian Vuia 1-4, RO-320085 Resita
ROMANIA
d.frunzaverde@uem.ro; http://www.cchapt.ro/
VIOREL CÂMPIAN
Center for Research in Hydraulics, Automation and Thermal Processes – CCHAPT
"Eftimie Murgu" University of Resita
P-ta Traian Vuia 1-4, RO-320085 Resita
ROMANIA
v.campian@uem.ro; http://www.cchapt.ro/
DORIAN NEDELCU
Center for Research in Hydraulics, Automation and Thermal Processes – CCHAPT
"Eftimie Murgu" University of Resita
P-ta Traian Vuia 1-4, RO-320085 Resita
ROMANIA
d.nedelcu@uem.ro; http://www.cchapt.ro/
GILBERT-RAINER GILLICH
Center of Advanced Research, Design and Technology – CARDT
"Eftimie Murgu" University of Resita
P-ta Traian Vuia 1-4, RO-320085 Resita
ROMANIA
gr.gillich@uem.ro; http://www.cardt.ro/
GABRIELA MĂRGINEAN
Laboratory for Material Science and Material Testing
University of Applied Sciences Gelsenkirchen
Neidenburger Str. 10, D-45877 Gelsenkirchen
gabriela.marginean@fh-gelsenkirchen.de; http://www.fh-gelsenkirchen.de/

Abstract: The paper presents the results of the failure analysis of a Kaplan turbine runner blade from a hydropower station in Romania. In order to determine the causes that led to the crack, the authors carried out metallographic investigations on a sample obtained from the damaged blade. They led to the conclusion, that the cracking of the blade was caused by fatigue, initiated by the numerous non metallic inclusions, which were discovered in the vicinity of the blade surface. The results obtained by metallographic investigations were completed by numerical analysis regarding the resistance of the blade and service life estimations. The calculations showed that the cracking of the blade started and developed from the stress concentrator placed between the blade and blade flange. In order to avoid further damages, the blade geometry and the number of blades have to be reconsidered.

Key-Words: Hydropower station, Kaplan turbine, fatigue cracking, service life estimations

1 Introduction

Hydro turbine components are exposed to high mechanical loadings and corrosion. Fatigue, erosion and cavitation are the main factors which may lead to failure and therefore to expensive maintenance activities.

The analysis regarding the working conditions showed that the cracking occurred (Fig. 1) in one of

the turbines from hydropower plants cascade, which operated at a higher head than the rest.

Fig.1 The cracked runner blade

The technical characteristics of the damaged turbine are:

- ✓ runner diameter - 5500 mm
- ✓ nominal speed - 115.4 rpm
- ✓ maximum power for net head - 35.5 MW
- ✓ maximum head - 28.20 m
- ✓ net head - 24.0 m
- ✓ minimum head - 16.0 m

Fig.2 shows the path of the investigated crack, which penetrated the blade and developed to a final length of 600 mm, measured on the pressure side.

Fig.2 The crack on the pressure side

2 Methodology

In order to define the causes that led to the failure of the blade, the authors carried out both metallographic investigations and numerical analysis regarding the resistance of the blade and service life estimations.

2.1 Metallographic Investigations

The sample for metallographic investigations was cut from the cracked blade as indicated in Fig.3.

Fig.3 Position of the metallographic sample

The macroscopic examination of the fracture surface (Fig. 4), revealed the specific appearance of fatigue cracking [1]. The surface is smoothened, resulting from the relative friction of the two pieces of the cracked blade one upon the other, during the alternative loads. The positions of the fan-shaped striations indicate that the cracking started from the region marked with “SP” (starting point) in Fig.4 The SEM-micrographs of the regions marked with “a” and “b” are presented in Fig.5.

Fig.4 Macrograph of the fracture surface

The images shown in Fig.5 indicate a high content of non-metallic inclusions in the blade material (marked with 1 in Fig.5.a). During the crack propagation, the operating water determined the corrosion of the base material surrounding these inclusions. As a consequence, the non-metallic inclusions released from the surface, leaving craters behind (position 2 in Fig.5.b), which were filled in with corrosion products (position 3 in Fig. 5.b).

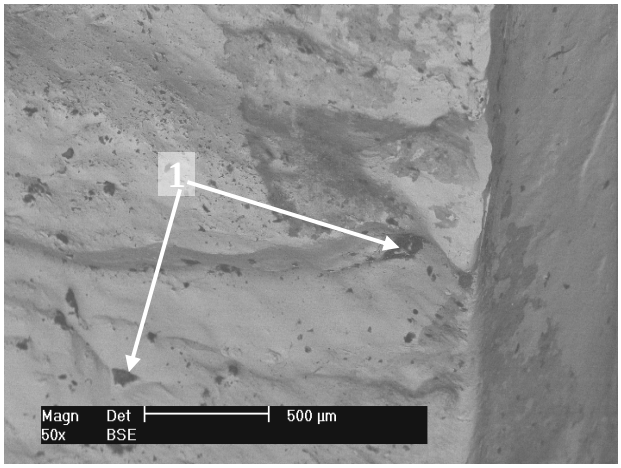

a – BSE-image, 50x

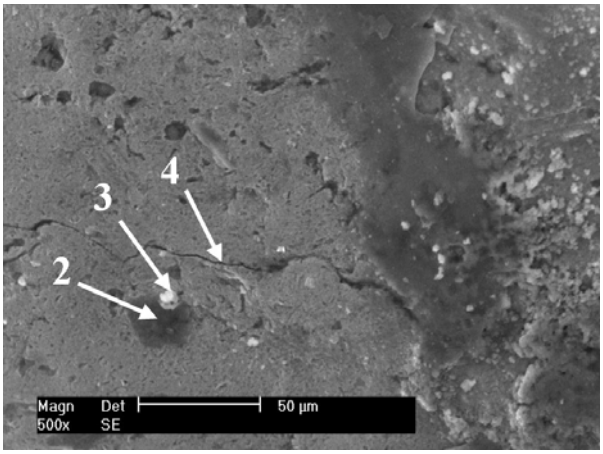

b – SE-image, 500x

Fig.5 SEM-micrographs of the fracture surface

In the surface of the investigated sample numerous secondary cracks (as marked by 4 in Fig.5.b) were observed, which are specific for fatigue cracking [2], [3].

After SEM-examination, the crack surface was grinded, polished and examined with the scanning electron microscope (Philips XL30 ESEM). Globular non-metallic inclusions could be observed, as well as the surrounding corrosion attack of the metallic material (Fig.6.a). The XRD-analyze led to the conclusion, that these inclusions are silicates and oxides (Fig.6.b).

In order to visualize the structure of the blade material, the sample was etched using a V2A-solution and was examined with the light microscope (LEICA DM 6000M). As shown in Fig.7, the microstructure is consisting of martensite, containing a high percentage of ferrite, with grid-like distribution. The presence of numerous non-metallic inclusions is attested also by these images.

The metallographic investigations led to the conclusion that the cracking of the blade was caused by fatigue and was initiated by non metallic inclusions existing in the vicinity of the blade surface. The crack propagation occurred gradually, through development of the principal fracture front. Because of the high content of non-metallic inclusions and the inhomogeneous structure of the blade material, additionally numerous secondary cracks developed inside the material.

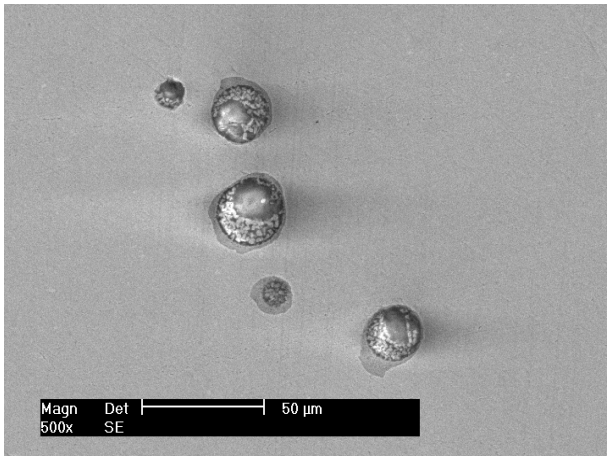

a - SEM-micrograph

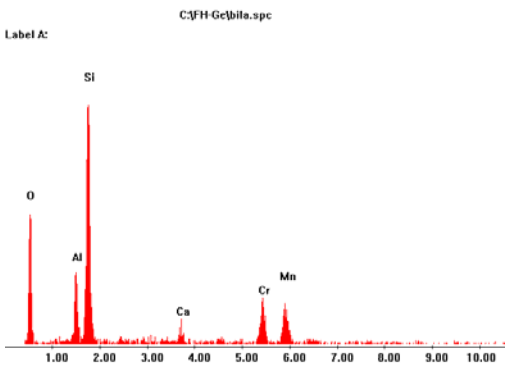

b - XRD-capture of the inclusions

Fig.6 Non-metallic inclusions in the vicinity of the crack surface

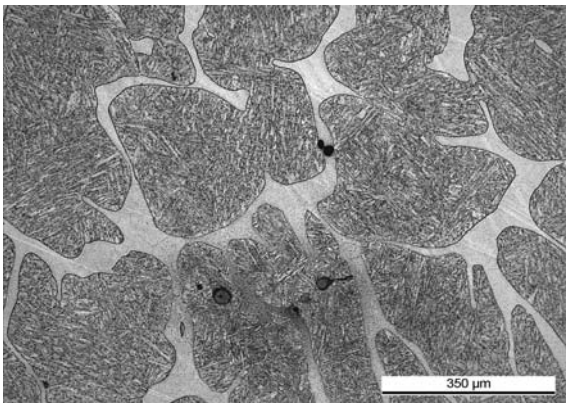

a – 200x

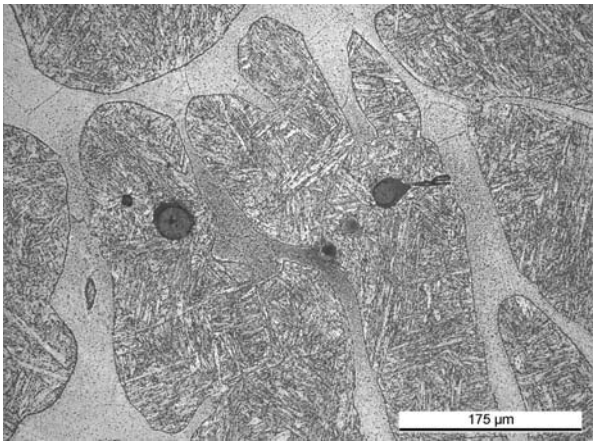

b – 500x

Fig.7 Structure of the blade material

After the failure was initiated, the fracture surfaces were exposed to chemical corrosion. This phenomenon was accentuated and accelerated by the presence of the high content of non metallic inclusions.

2.2 Calculations Regarding the Resistance and Service Life Estimations of the Blade

The calculations of the blade included the following steps:

- the 3D solid modeling of the runner blade, using the Autodesk Inventor software;
- determination of the blade loads starting from hydrodynamic conditions;
- linear static analyses, for different stress relieve groove geometries and blade numbers;
- service life estimations, calculated for maximal stress values of the concentrators resulted from the COSMOS Design Star software, using the Haigh fatigue diagram.

The axial blade turbine has a very complex geometry, which must be generated in a Computer Aided Software (CAD) for the final blade drawing and for finite elements resistance calculations. Autodesk Inventor was chosen as CAD software. The purpose of the modelling process is to obtain the blade as a solid object and not as a surface, so that it may be used for finite elements resistance calculations. Therefore the following steps are required:

- generation of the suction side surface, pressure side surface and leading edge surface, based on closed loops of the 3D coordinates disposed on cylinders;
- extensions of blade's surfaces: the previous surfaces must be extended to the hub and periphery direction to obtain the surfaces of the complete blade;
- intersections of the blade surfaces with radial planes, disposed at imposed angles, which will generate a number of closed loops disposed on radial planes;
- generation of the solid model of the blade, based on the previous closed loops;
- completion of the 3D solid geometry of the blade with the flange and stress relieve groove with different geometry, Fig.8 and Fig.9.

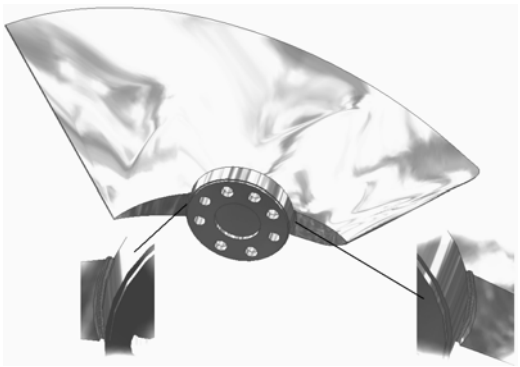

Fig.8 The solid model of the blade with stress relieve groove R8x20

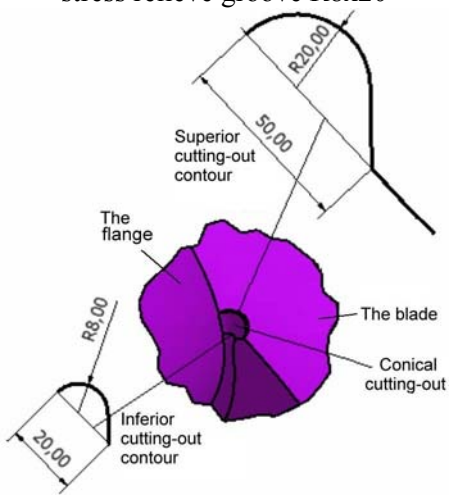

Fig.9 The geometry of the stress relieve groove R20x50

The hydrodynamic loads applied on the axial runner are presented in Fig.10:

- the gravity load $\vec{G}$;
- the centrifugal force $\overrightarrow{F_C}$ for the runner speed 115.4 rot/min;
- the axial thrust $\overrightarrow{F_{AH}}$, resulted from the measurements on model;

- the tangential force $\overrightarrow{F_T}$,
- $\vec{R}$ is the resultant of the hydraulic force on the blade
- "e" is the distance to the blade axis.

The operation points considered for resistance calculus correspond to the following power values: 35.5 MW, 30 MW, 25 MW, 20 MW and 15 MW at different head values. The axial thrust and tangential forces were calculated for 4 and 6 runner blades. The placement of the operating points in the prototype hill chart is shown in Fig.11.

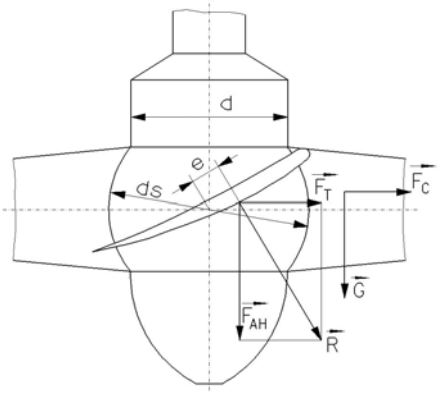

Fig.10 The hydrodynamic loads applied to the runner

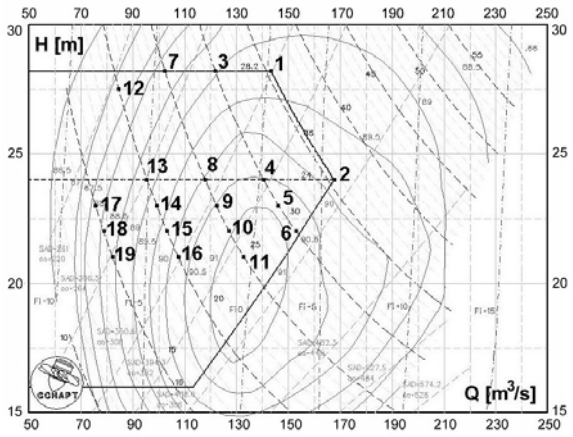

Fig.11 The placement of the operating points in the prototype hill chart

The numerical study was made with the Cosmos Design Star software, which offers a wide range of advanced type analyses: linear static analysis and nonlinear analysis, frequency analysis, linearized buckling analysis and thermal analysis.

Fig.12 shows the loads and restrictions applied to the blade:

- Fixed type constraints applied to the flange holes, which impose 0 value for the translations and rotations of the selected entities; axial thrust FAH;
- tangential force FT;
- centrifugal force Fc;
- blade gravity G.

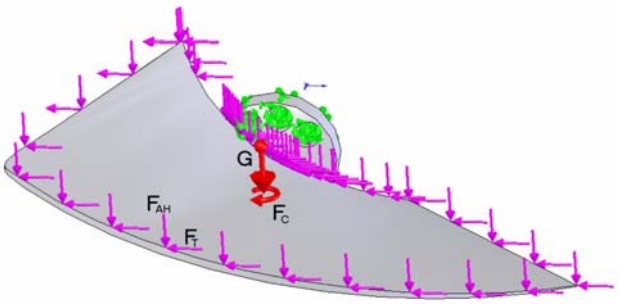

Fig.12 Loads and restrictions applied to the blade

Because the blade cannot be generated as a surface with constant thickness, for finite element analyse, only solid mesh (parabolic tetrahedral solid elements) can be used. The mesh is shown in Figure 13. For original stress relieve groove R8x20 a local fine mesh was used, Figure 14. The results are presented numerically in Table 1, and graphically in Figure 15 and Figure 16, only for operating point no. 1.

Fig.13 The blade mesh

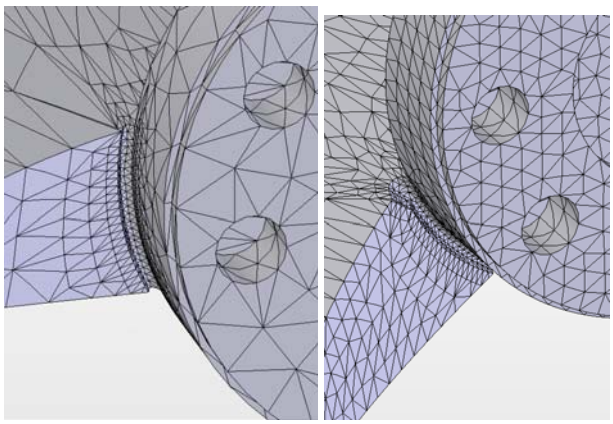

Fig.14 The blade mesh in the stress relieve groove area

Table 1 Numerical results for stress relieve groove R8x20 (4 blades)

Operation point	Head H [m]	Power P [MW]	Von Mises Stress	Max. Displacement
1	28.2	35.5	474.7	20.47
2	24	35.5	434	17.97
3	28.2	30	467.7	20.27
4	24	30	447.5	17.55
7	28.2	25	475.4	19.32
8	24	25	444.6	17.57
12	27.5	20	472.7	19.35
13	24	20	443.6	17.7
17	23	15	426.4	16.91

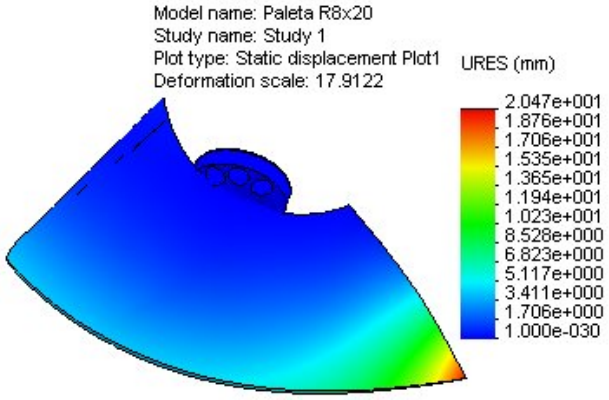

Fig.15 The resultant displacement plot

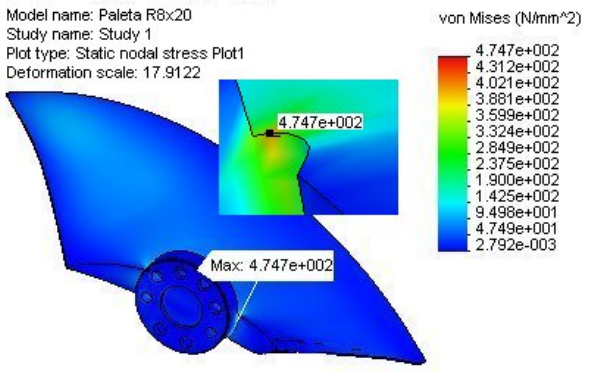

Fig.16 The Von Mises stress plot

To reduce the maximal stress values, the geometry of the stress relieve groove was modified from R8x20 to R20x50, Fig.9. The results are numerically shown in Table 2.

Table 2 presents a reducing of the Von Mises stress values for a power range of 30…15 MW, but not enough to promote the solution. In these circumstances, the blade loads can be reduced by blade number increasing. Table 3 shows the numerical results for stress relieve groove R8x20 with 6 blades. A significant decreasing of the stress and displacements values can be observed, comparing with the previous solutions.

Table 2 Numerical results for stress relieve groove R20x50 (4 blades)

Operation point	Head H [m]	Power P [MW]	Von Mises Stress	Max. Displacement
1	28.2	35.5	426.3	20.47
2	24	35.5	388.8	17.97
3	28.2	30	421.0	20.28
4	24	30	386.4	17.98
7	28.2	25	411.4	19.78
8	24	25	384.6	17.99
12	27.5	20	409.8	19.82
13	24	20	384.5	18.13
17	23	15	370.1	17.32

Table 3 Numerical results for stress relieve groove R20x50 (6 blades)

Operation point	Head H [m]	Power P [MW]	Von Mises Stress	Max. Displacement
1	28.2	35.5	357.3	13.76
2	24	35.5	330.0	12.09
3	28.2	30	352.7	13.63
4	24	30	339.9	11.82
7	28.2	25	358.4	12.99
8	24	25	337.9	11.83
12	27.5	20	356.6	13.01
13	24	20	337.3	11.92
17	23	15	325.8	11.39

For service life estimations a standard procedure for hydraulic turbine is used, for the operating points with maximal stress values. The amplitude oscillation for Kaplan blade turbine is experimentally obtained and is around 20 MPa. The yield strength value of the blade material is $R_{P0,2\ min}$=550 MPa. The calculated values of the stress for stress relieve groove R8x20 and R20x50 and 4 blades were introduced in Haigh diagram, Fig. 17 [4].

From the Haigh diagram results that, for stress relieve groove R8x20, the blade cracks should be obtained between $10^9 \div 10^{10}$ of the fatigue cycles. To reduce the stress concentrator values, a number of different stress relieve groove geometry were studied. The optimal solution was obtained for stress relieve groove R20x50, where the stress values were reduced in the range between 45...60 MPa (see

Table 2 and Fig. 17), but not enough to promote as a final solution.

The results from Fig.17 are ideally, because the fatigue curves are obtained in laboratory for samples with controlled chemical composition and homogeneity, with no fissures and surfaces or deeply defects. For these reasons, in service life estimations and fatigue calculus is recommended that the stress concentrator values will not be higher than half of yield strength value of the material, in our case 275 MPa.

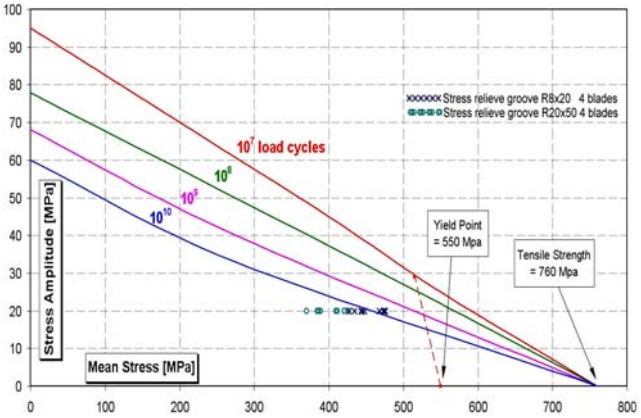

Fig.17 The Haigh diagram

4 Conclusions

The metallographic investigations and the calculations carried out led to the conclusion that the cracking of the blade started and developed from the stress concentrator placed between blade and blade flange on the leading edge direction.

A few stress relieve groove geometry were analysed, but did not generate a decreasing of the stress concentrators in admissible limits (smaller than half of yield strength value of the material). This effect cannot be obtained only by modifying the stress relieve groove geometry.

In order to decrease the maximal stress value it is necessary to reduce the hydrodynamic loads on the blade. For existing operating conditions (discharge, head, speed, power), the stress decreasing is possible only by increasing the number of the runner blades.

In order to verify this conclusion, for the same blade geometry, a blade with stress relieve groove R8x20 was calculated, but for 6 blades. The results show a significant decreasing of the stress concentrators values (about 100 MPa) which, associated with an optimal stress relieve groove geometry, can lead to a stress reducing in admissible limits. These calculations are theoretically, because they are made for a runner with 6 blades and the same geometry of the blade. But, a new runner, with 5 or 6 blades, will require a new blade geometry (new profiles, a blade with a smaller extensions), and, therefore, the loads will be modified.

Acknowledgement

The work has been supported by the MATNANTECH program, project CEEX-M1-C2-1185, Contract no. 64/2006, acronym iSMART-flow. Numerical computations and experimental investigations have been performed at the ExpertLAB from the Research Centre for Hydraulics, Automation and Thermal Processes, „Eftimie Murgu" University of Reşiţa, www.cchapt.ro.

References:

[1] X1. Lange G., *Systematische Beurteilung technischer Schadensfälle*, *5.Auflage,* Wiley - VCH Verlag, D-69469 Weinheim, Germany, 2001, pp. 103-147.

[2] X1. Lange G., *Systematische Beurteilung technischer Schadensfälle*, *5.Auflage,* Wiley - VCH Verlag, D-69469 Weinheim, Germany, 2001, pp.163

[3] X2. Schmidt P.F., *Praxis der Rasterelektronen-mikroskopie und Mikrobereichsanalyse*, Expert Verlag, Renningen - Malmsheim, Germany, 1994, pp. 103-147

[4] X3. Keck Helmuth, *Stakeholders perspectives on the challenges or threats and on "A European research network as one instrument to effective rehabilitation and utilization of European hydropower Infrastructure"*, Elforsk Workshop, Stockholm, Sweden, June 29th 2004